



**HAL**  
open science

## Copper line transmission and communication

Charbel Tannous

► **To cite this version:**

Charbel Tannous. Copper line transmission and communication. Master. Technologies des Médias, UBO Brest, France. 2015, pp.25. hal-04545609

**HAL Id: hal-04545609**

**<https://hal.science/hal-04545609>**

Submitted on 14 Apr 2024

**HAL** is a multi-disciplinary open access archive for the deposit and dissemination of scientific research documents, whether they are published or not. The documents may come from teaching and research institutions in France or abroad, or from public or private research centers.

L'archive ouverte pluridisciplinaire **HAL**, est destinée au dépôt et à la diffusion de documents scientifiques de niveau recherche, publiés ou non, émanant des établissements d'enseignement et de recherche français ou étrangers, des laboratoires publics ou privés.

# Copper line transmission and communication

C. Tannous 

*Université de Brest, Lab-STICC, CNRS-UMR 6285, F-29200 Brest, FRANCE*

(Dated: [April 14, 2024](#))

Development of wired telecommunications and Internet benefited from the deep knowledge of copper cables and later on fiber optics. We describe the development of copper cables to highlight the notions of bandwidth, quality factor, communication speed... and their impact on present communication technologies.

PACS numbers: 84.70.+p, 84.40.Az, 84.40.Ua, 89.70.-a

Keywords: Transmission lines and cables, Transmission lines, telecommunications, Theory of telecommunications

## Contents

|  |    |
|--|----|
| <b>I. Introduction</b>                                       | 1  |
| <b>II. Linear Time-Invariant Systems</b>                     | 3  |
| A. Impulse response function                                 | 3  |
| 1. Impulse response determination                            | 4  |
| B. LTI System Causality and Stability                        | 4  |
| C. Transfer Function   | 5  |
| 1. Laplace transform: Complex Angular Frequency response     | 5  |
| 2. Fourier transform: Angular Frequency response             | 6  |
| D. Bandwidth   | 7  |
| E. Quality factor  | 8  |
| <b>III. Physical description of a transmission line</b>      | 10 |
| A. Telegrapher equations                                     | 11 |
| B. Complex Propagation                                       | 12 |
| C. Gauge   | 13 |
| D. EMI filtering   | 14 |
| E. Joining cables of different symmetries: Balun transformer | 14 |
| <b>IV. Transmission line in telecommunications</b>           | 15 |
| A. Transfer function $H(f, d)$ versus communication distance | 15 |
| B. Crosstalk   | 16 |
| C. Cable Termination   | 18 |
| D. Secure communications                                     | 18 |
| <b>A. Cable Primary Constants</b>                            | 20 |
| <b>B. Laplace Transform of typical Signals</b>               | 21 |
| <b>C. Fourier transform of typical signals</b>               | 23 |
| <b>References</b>  | 25 |

## I. INTRODUCTION

Foundations of communications technology result from discoveries of the early 19th century great physicists such as Oersted, Ampère, Faraday, Henry [1, 2]...

The telegraph was invented seventeen years after the discovery of electromagnetism by Oersted in 1820. In spite of this great spinoff, much of the early work on communications was done by free-lance pioneering inventors, such as Morse, Bell, Edison, Tesla...

The telegraph is an electro-mechanical system that did not require development of new scientific principles to expand commercially in the mid 19th century. Nevertheless, the dot-dash code developed by Morse for the telegraph can be considered as one of the early digital communication breakthroughs.

Tighter interaction between physics and communications began quickly after the telephone [1, 2] invention by Alexander Graham Bell in 1876. Bell invented also twisted pair copper wires that make the basic components of analog telephone cables as well as of many types of analog and digital communication cables to be discussed further below.

Over the next century, physics research in communications while improving the technology [1, 2] managed to obtain fundamental results of interest to the entire physics community. In particular, the creation of Bell Telephone Laboratories (Bell Labs) in 1925 resulted in a tremendously important number of breakthroughs in Science, Physics as well as in Electrical & Communication Engineering such as the FAX (invented the same year in 1925), the Transistor, the Semiconductor Laser [1, 2]...

A non-exhaustive listing of some important inventions made by Bell Labs is given below:

- Nyquist: Sampling theorem and Intersymbol Interference
- Cooley and Tukey: Fast Fourier Transform
- Shannon: Information and rate distortion theories
- Bardeen, Brattain and Shockley: Bipolar Junction Transistor
- Heilmeier: Liquid Crystal Display
- Lucky: Equalization
- Kernigan and Ritchie: C computer language
- Thompson and Ritchie: UNIX Operating System
- Stroustrup: C++ language
- Sze: Floating Gate Transistor (Flash technology used in USB keys, Solid State Drives...)

Generally, four broad eras of physics impacted communications:

- Electromagnetism era (starting in 1820);
- Electron era (starting in 1897);
- Quantum mechanics era (starting in the 1920s);
- Quantum optics era (starting in 1958).

transforming the respective centuries into:

- 19th century of Electromagnetism: Copper wiring for electric power distribution, outdoor lighting, wired communication...
- 20th century of the Electron: Development of micro/nano electronics, computing, wired and wireless communications...
- 21st century of the Photon: Fiber optic communication, quantum information processing, computing and communication...

**Note:** Wireless communication issues are outside the scope of these lectures.

## II. LINEAR TIME-INVARIANT SYSTEMS

A general system (mechanical, electrical, chemical...) is symbolically represented by the relationship [3] between its time-dependent input  $x(t)$  and output  $y(t)$ :

$$y(t) = \mathcal{O}[x(t)]$$

where  $x(t)$  and  $y(t)$  are, respectively, the input (excitation) and output (response).  $\mathcal{O}[\ ]$  represents the operation imposed on the input signal by the system.

The system is linear if its input-output relationship satisfies both homogeneity and superposition. Specifically, let  $y(t)$  be the response of a system to an input  $x(t)$ , then

- Homogeneity:

$$\mathcal{O}[ax(t)] = a \mathcal{O}[x(t)] = a y(t)$$

(where  $a$  is a constant scalar)

- Superposition:

$$\mathcal{O}\left[\sum_{i=1}^n x_i(t)\right] = \sum_{i=1}^n \mathcal{O}[x_i(t)] = \sum_{i=1}^n y_i(t)$$

(where  $y_i(t) = \mathcal{O}[x_i(t)]$ )

These properties require the following:

$$\mathcal{O}\left[\sum_{i=1}^n a_i x_i(t)\right] = \sum_{i=1}^n a_i \mathcal{O}[x_i(t)] = \sum_{i=1}^n a_i y_i(t)$$

A system is time-invariant when:

$$\mathcal{O}[x(t)] = y(t), \quad \text{implies} \quad \mathcal{O}[x(t - \tau)] = y(t - \tau)$$

### A. Impulse response function

In telecommunication, an input signal (message)  $x(t)$  at time  $t$  goes through a channel and emerges from it (cf. Fig. 1) as an output  $y(t)$ .

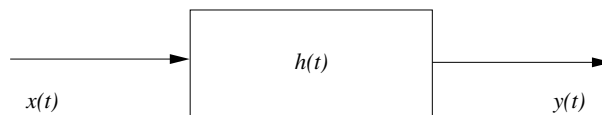


**Fig.1:** Impulse response of a signal  $x(t)$  (input voltage) and output signal  $y(t)$  with  $h(t)$  the impulse response relating them.

In a linear channel, input and output [3] are related by:

$$y(t) = \int_{-\infty}^{\infty} x(t')h(t, t')dt' \quad (1)$$

Exploiting time-invariance of the system from relation  $h(t, t') = h(t - t')$ , the operator  $\mathcal{O}[\cdot]$  representing the system effect on its input is transformed into a convolution operation (\*) [3] of  $x(t)$  and  $h(t)$  functions as:

$$y(t) = \int_{-\infty}^{\infty} x(\tau)h(t - \tau)d\tau = x(t) * h(t), \quad \text{or} \quad y(t) = \int_{-\infty}^{\infty} h(\tau)x(t - \tau)d\tau = h(t) * x(t) \quad (2)$$

In other words, a message  $x(t)$  transmitted through a LTI medium is convoluted with the channel impulse response  $h(t)$  resulting in an output message  $y(t)$ .

Note that in the most general case, a non-linear time-dependent [4] communication channel described as a scalar input-output relationship might be viewed mathematically as an expression  $y(t) = F[x(t)]$  with input  $x(t)$  and output  $y(t)$  where  $F$  is a non-linear functional that depends in general on  $x(t)$  as well as its higher order time derivatives  $x'(t), x''(t)...$

In the simple case, when  $F[x(t)]$  depends only on  $x(t)$ , the Volterra expansion entails expressing the response  $y(t)$  versus  $x(t)$  in the form of a series expansion with the help of generalized impulse response functions  $h_1, h_2, h_3...h_n$  taken at different times  $t_1, t_2...$  in the following way:

$$y(t) = \int_{-\infty}^{\infty} h_1(t, t_1)x(t_1)dt_1 + \iint_{-\infty}^{\infty} h_2(t, t_1, t_2)x(t_1)x(t_2)dt_1dt_2 + \iiint_{-\infty}^{\infty} h_3(t, t_1, t_2, t_3)x(t_1)x(t_2)x(t_3)dt_1dt_2dt_3... \quad (3)$$

### 1. Impulse response determination

Impulse response  $h(t)$  evaluation of any communication channel is done by sending through the channel a Pseudo-Random signal  $x(t)$  whose auto-correlation is a Dirac delta function that allows to identify  $h(t)$  at the receiver since:

$$h(t) = \int_{-\infty}^{\infty} h(t-t')\delta(t')dt' \quad (4)$$

Note that the word pseudo qualifies a signal that can be reproduced at will exactly for controllability reasons in contrast to a true random signal that is generally not reproducible.

In a digital framework the continuous Pseudo-Random signal  $x(t)$  is transformed into a Pseudo-Random Binary Sequence (PRBS) [5] consisting of sequences of 0 and 1.

When the impulse response  $h(t)$  is determined with a PRBS, it is known to be immune to distortion. This is why despite the fact, many other methods [6] exist to measure  $h(t)$  with various degrees of success, PRBS is still preferred when distortion is an issue.

A PRBS  $x[k]$  ( $k$  being an integer) is a balanced sequence made from equally probable symbols with values  $\pm 1$  such that the PRBS averages to zero. Choosing  $x[k] = (-1)^{a[k]}$  with  $a[k] = 0$  or 1 originating from a PRBS yields the desired values  $x[k] = \pm 1$  are equally probable.

The PRBS has many attractive features in addition to the balanced character: its standard deviation and peak values are both equal to 1 making its crest factor (largest value/standard deviation) equal to 1, the lowest value it can get [5]. PRBS having this noise-immune property [5] is required in communication electronics.

Note that PRBS are used not only in impulse response determination but also in secure communications, communication channel testing, synchronization of digital sequences (cf. section [IV D](#))...

## B. LTI System Causality and Stability

### • Causality

An LTI system is causal if its output  $y(t)$  depends only on current and past input  $x(t)$ . Assuming the system is initially at rest,  $y(t) = 0$ , its impulse response [3]  $h(t) = \mathcal{O}[\delta(t)]$  is zero for  $t < 0$ , and the response  $y(t)$  to an arbitrary input  $x(t)$  is:

$$y(t) = h(t) * x(t) = \int_{-\infty}^{\infty} h(\tau)x(t-\tau)d\tau = \int_0^{\infty} h(\tau)x(t-\tau)d\tau$$

Moreover, if the input begins at a specific moment, e.g.,  $x(t) = 0$  for  $t < 0$ , then we have

$$y(t) = h(t) * x(t) = \int_{-\infty}^{\infty} h(\tau)x(t-\tau)d\tau = \int_0^t h(\tau)x(t-\tau)d\tau$$

### • Stability

An LTI system is stable if every bounded input produces a bounded output, i.e.,

$$\text{if } |x(t)| < x_{max} \text{ then } |y(t)| < y_{max}$$

is true  $\forall t$ . But as the output and input of an LTI is related by convolution, we have:

$$\begin{aligned} |y(t)| &= \left| \int_{-\infty}^{\infty} h(\tau)x(t-\tau)d\tau \right| \leq \int_{-\infty}^{\infty} |h(\tau)x(t-\tau)|d\tau \\ &\leq \int_{-\infty}^{\infty} |h(\tau)||x(t-\tau)|d\tau < x_{max} \int_{-\infty}^{\infty} |h(\tau)|d\tau < y_{max} \end{aligned}$$

implying:

$$\int_{-\infty}^{\infty} |h(\tau)|d\tau < \infty$$

Thus an LTI system is stable if its impulse response function  $h(t)$  is absolutely integrable.

### C. Transfer Function

- **Continuous LTI system:**

1. *Laplace transform: Complex Angular Frequency response*

The transfer function of a filter considered as an LTI is most often defined in a complex angular frequency plane  $s = \sigma + j\omega$ .

The transfer function  $H(s)$  of a filter is the ratio of the output signal  $Y(s)$  to that of the input signal  $X(s)$  as a function of the complex angular frequency  $s$ :

$$H(s) = \frac{Y(s)}{X(s)}, \quad (5)$$

The transfer function of all linear time-invariant filters generally share certain characteristics:

For filters which are constructed of discrete components, their transfer function must be the ratio of two polynomials in  $s$ , i.e. a rational function of  $s$ . The transfer function order is the highest power of  $s$  encountered in either the numerator or the denominator.

All transfer function polynomials have real coefficients. Therefore, poles and zeroes of the transfer function are real or complex conjugate pairs.

Since filters are assumed to be stable, the real part of all poles (i.e. denominator zeroes) are negative, i.e. they lie in the left half-plane of complex frequency space.

Transfer functions of filters made of distributed elements (defined in section III) are not, in general, rational functions but can often be represented by them after some special transformations.

The proper construction of a transfer function involves the Laplace transform, and therefore it is needed to assume null initial conditions, since:

$$\mathcal{L} \left\{ \frac{df}{dt} \right\} = s \cdot \mathcal{L} \{f(t)\} - f(0), \quad (6)$$

And when  $f(0) = 0$  we can get rid of the constants and use the usual expression:

$$\mathcal{L} \left\{ \frac{df}{dt} \right\} = s \cdot \mathcal{L} \{f(t)\} \quad (7)$$

An alternative to transfer functions is to describe filter behavior as a convolution. The convolution theorem [7], valid for Laplace transforms, guarantees equivalence with transfer functions.

2. Fourier transform: Angular Frequency response

Assume the input signal is a complex exponential  $x(t) = e^{st}$ , where  $s = \sigma + j\omega$ , then the output of the LTI system [3] is

$$y(t) = \mathcal{O}[x(t)] = h(t) * x(t) = \int_{-\infty}^{\infty} h(\tau) e^{s(t-\tau)} d\tau = e^{st} \int_{-\infty}^{\infty} h(\tau) e^{-s\tau} d\tau = e^{st} H(s)$$

where

$$H(s) = \int_{-\infty}^{\infty} h(\tau) e^{-s\tau} d\tau$$

is the transfer function of the system.

- **Discrete LTI system:** Assume the input signal is a complex exponential  $x[n] = e^{sn} = z^n$ , where  $z = e^s$ , then the output of the LTI system is

$$y[n] = \mathcal{O}[x[n]] = h[n] * x[n] = \sum_{m=-\infty}^{\infty} h[m] z^{n-m} = z^n \sum_{m=-\infty}^{\infty} h[m] z^{-m} = z^n H(z)$$

where

$$H(z) = \sum_{m=-\infty}^{\infty} h[m] z^{-m}$$

is the transfer function of the system.

For any output-input relation  $y = \mathcal{O}[x]$ , when  $\mathcal{O}[x] = \lambda \cdot x$  the input  $x$  is eigenfunction of  $\mathcal{O}$  and  $\lambda$  is the corresponding eigenvalue.

Therefore the complex exponential input ( $e^{st}$  or  $e^{sn} = z^n$ ) is the eigenfunction of any LTI system, the transfer function ( $H(s)$  or  $H(z)$ ) is eigenvalue of the LTI system.

Transfer function ( $H(s)$  or  $H(z)$ ) is defined over a 2D complex plane ( $s$  or  $z = e^s$ ). In addition, when  $\sigma = 0$ , i.e.,  $s = j\omega$  and  $z = e^{j\omega}$ , the transfer function becomes an angular frequency response function

$$H(j\omega) = \int_{-\infty}^{\infty} h(t) e^{-j\omega t} dt$$

and

$$H(e^{j\omega}) = \sum_{m=-\infty}^{\infty} h[m] e^{-j\omega n}$$

Note that  $H(j\omega)$  is  $H(s)$  evaluated along vertical axis  $s = j\omega$ , and  $H(e^{j\omega})$  is  $H(z)$  evaluated along unit circle  $z = e^{j\omega}$ .

Consider in particular the system response to a complex exponential input  $x(t) = e^{j\omega t}$ :

$$y(t) = \mathcal{O}[e^{j\omega t}] = h(t) * e^{j\omega t} = \int_{-\infty}^{\infty} h(\tau) e^{j\omega(t-\tau)} d\tau = e^{j\omega t} \int_{-\infty}^{\infty} h(\tau) e^{-j\omega\tau} d\tau = H(\omega) e^{j\omega t}$$

where

$$H(\omega) = \int_{-\infty}^{\infty} h(\tau) e^{-j\omega\tau} d\tau = \mathcal{F}[h(t)]$$

is the frequency response function, which is the Fourier transform of the impulse response function.  $H(j\omega)$  is the eigenvalue of the LTI system and  $e^{j\omega t}$  is the corresponding eigenfunction:

$$\mathcal{O}[e^{j\omega t}] = H(\omega) e^{j\omega t}$$

This result can be generated to an arbitrary input as a linear combination of complex exponentials of different frequencies  $\omega$ :

$$x(t) = \frac{1}{2\pi} \int_{-\infty}^{\infty} X(\omega) e^{j\omega t} d\omega = \int_{-\infty}^{\infty} X(\omega) e^{j2\pi f t} df = \mathcal{F}^{-1}[X(\omega)]$$

The system response to this input is:

$$y(t) = \mathcal{O}[x(t)] = \mathcal{O} \left[ \int_{-\infty}^{\infty} X(\omega) e^{j\omega t} df \right] = \int_{-\infty}^{\infty} X(\omega) \mathcal{O} [e^{j\omega t}] df \quad (8)$$

This can be written as:

$$\int_{-\infty}^{\infty} X(\omega) H(\omega) e^{j\omega t} df = \int_{-\infty}^{\infty} Y(\omega) e^{j\omega t} df = \mathcal{F}^{-1} [Y(\omega)] \quad (9)$$

where

$$H(\omega) X(\omega) = Y(\omega) = \mathcal{F}[y(t)]$$

is the Fourier transform of response  $y(t)$ .

In summary, the output of an LTI system can be found

- in time domain by its impulse response  $h(t)$ :

$$y(t) = h(t) * x(t)$$

or, equivalently,

- in frequency domain by its frequency response  $H(\omega)$ :

$$Y(\omega) = H(\omega) X(\omega), \quad \text{or} \quad Y(f) = H(f) X(f)$$

This implies since these expressions are complex:

$$|Y(f)| = |H(f)| |X(f)|, \quad \arg(Y(f)) = \arg(H(f)) + \arg(X(f)) \quad (10)$$

meaning that output magnitude  $|Y(f)|$  is impacted by  $|H(f)|$  and output  $Y(f)$  is delayed by  $\arg(H(f))$  with respect to  $X(f)$ .

#### D. Bandwidth

Consider  $x(t)$  a single pulse displayed in Fig 2.

$x(t)$  Fourier transform is then:

$$X(f) = \int_{-\infty}^{\infty} x(t) e^{j2\pi f t} dt \quad (11)$$

This yields:

$$X(f) = \int_{-\tau/2}^{\tau/2} A e^{j2\pi f t} dt = \frac{A}{\pi f} \sin(\pi f \tau) \quad (12)$$

$X(f)$  modulus  $|X(f)| = \frac{A}{\pi} \left| \frac{\sin(\pi f \tau)}{f} \right|$  is displayed in Fig 2.

Evaluating power to half its value or 3dB drop (since  $10|\log_{10}(1/2)| = 3$ ), one has to find frequency  $f = B_S$  at which  $|X(f)|$  drops from  $A\tau$  to  $A\tau/\sqrt{2}$  (normalized amplitude dropping from de 1 to  $\frac{1}{\sqrt{2}}$  in Fig 2).

Thus we get the condition  $A \frac{\sin(\pi B_S \tau)}{\pi B_S} = \frac{A\tau}{\sqrt{2}}$ .

If we write  $B_S = \frac{1}{2\tau}$ , the condition becomes  $\frac{1}{\pi} = \frac{1}{2\sqrt{2}}$ .

Numerically  $\pi = 3.1415$  and  $2\sqrt{2} = 2.828$  meaning that the approximation  $B_S = \frac{1}{2\tau}$  is acceptable to  $\sim 10\%$ .

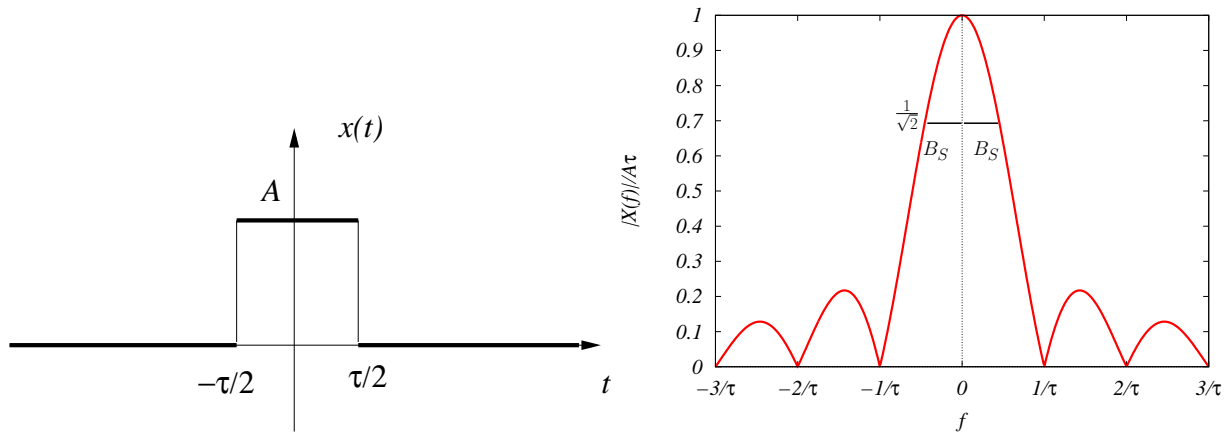


**Fig.2:** (left) Single pulse of duration  $\tau$ . (right) Fourier transform of  $x(t)$ . Bandwidth  $B_S$  is estimated from 3 dB drop in amplitude from 1 to  $\frac{1}{\sqrt{2}}$ .

### E. Quality factor

Quality factor  $Q$  is informally described from a resonant electric circuit or equivalently, a mechanical damped spring-mass oscillator with a classical equation of motion:

$$m \frac{d^2 x(t)}{dt^2} + 2m\lambda \frac{dx(t)}{dt} + m\omega_0^2 x(t) = 0 \quad (13)$$

$x(t)$  is displacement versus time,  $m$  is mass,  $\lambda$  is friction coefficient,  $\omega_0$  is the resonant angular frequency and  $m\omega_0^2$  is spring constant.

In the underdamped case (i.e. for  $\omega_0 > \lambda$ , then it is possible to define  $\omega = \sqrt{\omega_0^2 - \lambda^2}$ ), the solution of eq. 13 is:

$$x(t) = A_0 e^{-\lambda t} \cos(\omega t + \phi_0) = A_0 e^{-\frac{t}{\tau}} \cos(\omega t + \phi_0) \quad (14)$$

where  $\tau = 1/\lambda$  and  $A_0, \phi_0$  are initial amplitude and phase.

Oscillation nature and damping are characterized by the  $Q$  factor. Large  $Q$  describes lightly damped oscillations whereas a small  $Q$  characterizes heavier damped oscillations. There are nonetheless many other possibilities to define a Quality factor:

1.  $Q$  is real over twice imaginary frequency parts:

Given:  $x(t) = A_0 e^{-\frac{t}{\tau}} \cos(\omega t + \phi_0)$ , we rewrite it as  $x(t) = A_0 \text{Re}[e^{j(\omega' + j\omega'')t + j\phi_0}]$  by defining a complex angular frequency  $\omega' + j\omega''$  with  $\omega' = \omega$ , and  $\omega'' = \frac{1}{\tau}$ . Then  $Q = \frac{\omega'}{2\omega''}$  or  $Q = \frac{\omega\tau}{2} = \pi \frac{\tau}{T}$ .

In other words,  $Q$  is half oscillation angular frequency over damping coefficient.

Let us rewrite  $x(t) = A_0 e^{-\frac{t}{\tau}} \cos(\omega t + \phi_0)$  in terms of amplitude change  $\delta A$  leading to energy change  $\delta E$  over one cycle or period  $T$ .

Writing  $A = A_0 e^{-\frac{T}{\tau}}$  and  $\delta A = A_0 - A_0 e^{-\frac{T}{\tau}}$  to express amplitude change over a period gives for large  $Q$ ,

$$\frac{A}{\delta A} = \frac{A_0 e^{-\frac{T}{\tau}}}{A_0(1 - e^{-\frac{T}{\tau}})} \approx \frac{Q}{\pi} \quad (15)$$

Thus:

$$Q = \pi \frac{A}{\delta A} \quad (16)$$

Since stored energy  $E \propto A^2$  we get:

$$Q = 2\pi \frac{E}{\delta E} \quad (17)$$

since  $\delta E \propto (A + \delta A)^2 - A^2 \approx 2A\delta A$ .

This corresponds to the widely accepted value informally quoted as:

$$Q = 2\pi \frac{\text{Energy stored}}{\text{Energy dissipated per cycle}} \quad (18)$$

2.  $Q$  is decay time over period ratio:

$Q$  is then defined by:  $Q = 2\pi \frac{\tau}{T} = \omega\tau$  which is twice the previous value in order to tell how many periods fit in a single decay interval, or how many periods it takes for the oscillation to run out of energy.

Writing  $A = A_0 e^{-\frac{t}{\tau}}$  and  $\delta A = A_0 - A_0 e^{-\frac{T}{\tau}}$  to express amplitude change over a period gives for large  $Q$ ,

$$\frac{A}{\delta A} = \frac{A_0 e^{-\frac{2\pi}{Q}}}{A_0(1 - e^{-\frac{2\pi}{Q}})} \approx \frac{Q}{2\pi} \quad (19)$$

Thus we get twice the previous values:

$$Q = 2\pi \frac{A}{\delta A}, \quad Q = 4\pi \frac{E}{\delta E} \quad (20)$$

3.  $Q$  causes a shift of resonance frequency:

Using  $Q = 2\pi \frac{\tau}{T} = \omega\tau$  and  $\omega = \sqrt{\omega_0^2 - (\frac{1}{\tau})^2}$ , we get  $\omega \approx \omega_0(1 - \frac{1}{2Q^2})$  for large  $Q$ .

4.  $Q$  is a measure of resonance sharpness inversely proportional to bandwidth:

Resonance sharpness is an indicator of tuning quality of communication devices [8]. In order to illustrate this notion, we consider an  $R, L, C$  circuit which is equivalent to a mechanical damped oscillator.

A circuit element such as  $R, L, C$  is considered as lumped when the frequency is so low that an applied electromagnetic field wavelength  $\lambda$  applied to the element is such that  $\lambda \gg \ell$  where  $\ell$  is the typical length of the element. In the opposite case  $\lambda \ll \ell$  the circuit element is considered as distributed (cf. section III).

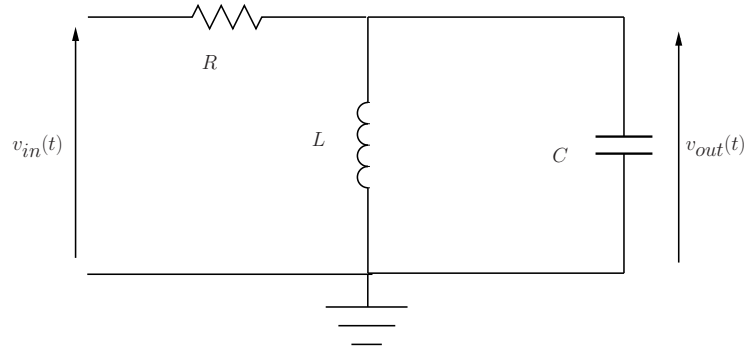


**Fig.3:** RLC circuit with an impedance  $Z = \frac{1}{R(jC\omega + \frac{1}{jL\omega}) + 1}$  relating output  $v_{out}(t)$  to input  $v_{in}(t)$  voltage.

According to Fig. 3 the output-input voltage ratio is given by:

$$\frac{V_{out}}{V_{in}} = \frac{1}{R(jC\omega + \frac{1}{jL\omega}) + 1} \quad (21)$$

where  $V_{out}, V_{in}$  are the Fourier Transforms of  $v_{out}(t), v_{in}(t)$ . Thus the transfer function (impedance) of the circuit is:

$$H(f) = \frac{1}{1 + jQ(\frac{f}{f_0} - \frac{f_0}{f})} \quad (22)$$

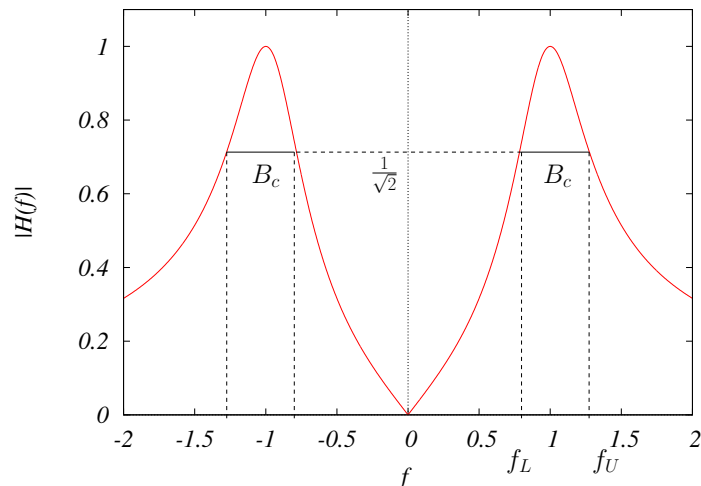


**Fig.4:** Transfer function  $|H(f)| = \frac{1}{|1+jQ(\frac{f}{f_0} - \frac{f_0}{f})|}$  with  $Q=2$  and  $f_0=1$ . The lower and upper frequencies  $f_L, f_U$  correspond to the 3 dB drop of  $|H(f)|$  from 1 to  $\frac{1}{\sqrt{2}}$  yielding the circuit bandwidth  $B_c = f_U - f_L$ .

where  $f_0 = 1/2\pi\sqrt{LC}$  is the resonance frequency and  $Q = R\sqrt{\frac{C}{L}}$ .

Given a 3 dB drop of  $|H(f)|$  from 1 to  $\frac{1}{\sqrt{2}}$  displayed in Fig. 4, we determine the cutoff frequencies  $f_L, f_U$  such that  $f_U - f_L = f_0/Q$  by solving the condition at 3 dB drop:  $|H(f)| = \frac{1}{\sqrt{2}}$  that is  $Q(\frac{f}{f_0} - \frac{f_0}{f}) = \pm 1$ . The solutions are:

$$\frac{f_L}{f_0} = \frac{-1/Q + \sqrt{1/Q^2 + 4}}{2}, \quad \frac{f_U}{f_0} = \frac{1/Q + \sqrt{1/Q^2 + 4}}{2} \quad (23)$$

Thus  $f_U - f_L = B_c = f_0/Q$  and  $Q = f_0/B_c$  or  $QB_c = f_0$  leading to a compromise between  $Q$  and  $B_c$  for fixed  $f_0$ .

Note that in order to conform with Fig. 2, circuit bandwidth  $B_c$  is equal to  $f_U - f_L$  as if it were half the bandwidth of signal bandwidth  $B_S$ . This is simply due to the fact the resonance frequency  $f_0 \neq 0$  in contrast with the pulse Fourier transform centered on zero frequency.

### III. PHYSICAL DESCRIPTION OF A TRANSMISSION LINE

A transmission line (TL) is a very rich notion at the foundations of transmission of signals and information.

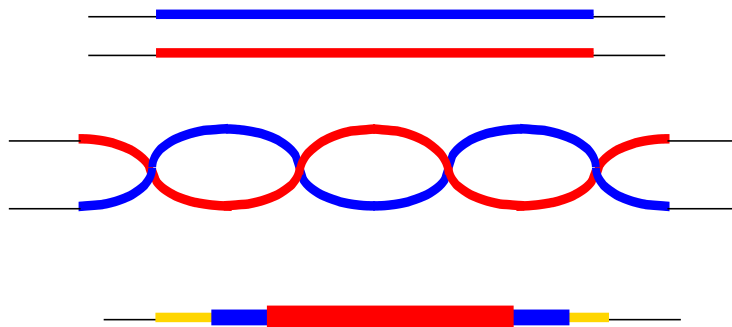


**Fig.5:** (Color on line) Straight Double wires, Twisted pair and Coaxial cable

There are many types of transmission lines:

1. Twisted pairs (TP) with almost confined fields (cf. Fig. 5) providing some shielding from external Electromagnetic Field Interference (EMI) originating from natural phenomena or radiation due to broadcast radio, TV... stations, GPS, Wi-Fi, Bluetooth, Cellphone emissions... Shielded TP or STP are protected by aluminum foils acting like a Faraday cage to provide additional protection against EMI.
2. Lecher wires or two-wire TL consisting of two parallel conductors
3. Coaxial cables (cf. Fig. 5) with well confined circular fields providing good shielding from EMI
4. Paired coaxial cables used in Video transmission
5. Computer cables: USB, Firewire, power, KVM (Keyboard, Video and Mouse) cables...
6. Microstrips, Coplanar lines, Striplines in Radio Frequency Integrated Circuits [9]
7. Trunk cables of bundled TP used in telephony consumer cabling
8. RF Waveguides

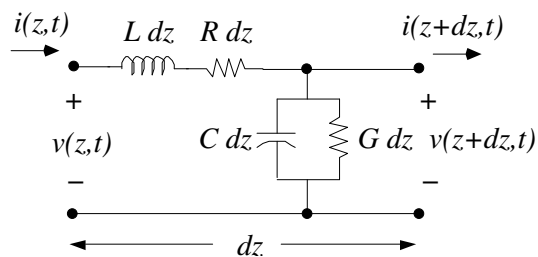


**Fig. 6:** Infinitesimal  $R, L, C, G$  section of a distributed description of a TL.

In a distributed description of a TL, consider a TL that has a series connection of inductance  $L$  (in H/m), a resistance  $R$  (in  $\Omega/m$ ), a parallel capacitance  $C$  (in F/m) and conductance  $G$  (in  $\Omega^{-1}/m$ ).

Thus taking an infinitesimal segment of line, having length  $dz$ , we have the circuit in Fig. 6.

### A. Telegrapher equations

1. Kirchoff Loop equation:

$$v(z, t) - R dz i(z, t) - L dz \frac{\partial i(z, t)}{\partial t} - v(z + dz, t) = 0$$

Divide by  $dz$ , and take the limit as  $dz \rightarrow 0$ :

$$-\frac{\partial v(z, t)}{\partial z} = R i(z, t) + L \frac{\partial i(z, t)}{\partial t}$$

2. Kirchoff Node equation:

$$i(z, t) - G dz v(z + dz, t) - C dz \frac{\partial v(z + dz, t)}{\partial t} - i(z + dz, t) = 0$$

Divide by  $dz$  and take the limit as  $dz \rightarrow 0$ :

$$-\frac{\partial i(z, t)}{\partial z} = G v(z, t) + C \frac{\partial v(z, t)}{\partial t}$$

Performing separation of variables  $z, t$  by adopting a time-harmonic evolution such that:  $v(z, t) = V(z)e^{j\omega t}$ ,  $i(z, t) = I(z)e^{j\omega t}$  yields:

$$-\frac{dV(z)}{dz} = (R + j\omega L)I(z), \quad -\frac{dI(z)}{dz} = (G + j\omega C)V(z) \quad (24)$$

Taking the derivative with respect to  $z$  and substituting we obtain second order (Wave) equations for  $V$  and  $I$ :

$$\frac{d^2V(z)}{dz^2} - \gamma^2V(z) = 0, \quad \frac{d^2I(z)}{dz^2} - \gamma^2I(z) = 0 \quad (25)$$

Solutions of Wave equations are:

$$V(z) = V_0^+ e^{-\gamma z} + V_0^- e^{\gamma z}, \quad I(z) = I_0^+ e^{-\gamma z} + I_0^- e^{\gamma z} \quad (26)$$

with:  $e^{-\gamma z}$  (resp.  $e^{\gamma z}$ ) representing forward (resp. backward) traveling wave

## B. Complex Propagation

- Propagation coefficient:  
 $\gamma = \sqrt{(R + j\omega L)(G + j\omega C)} = \alpha + j\beta$
- Attenuation coefficient:  
 $\alpha = \text{Re}[\sqrt{(R + j\omega L)(G + j\omega C)}]$
- Phase shift:  
 $\beta = \text{Im}[\sqrt{(R + j\omega L)(G + j\omega C)}]$
- Phase velocity:  $v_p = \omega/\beta = \omega/\text{Im}[\sqrt{(R + j\omega L)(G + j\omega C)}]$
- Characteristic Impedance  $Z_0$ :

$$\frac{dV(z)}{dz} = \frac{d[V_0^+ e^{-\gamma z} + V_0^- e^{\gamma z}]}{dz} = \gamma[-V_0^+ e^{-\gamma z} + V_0^- e^{\gamma z}] \quad (27)$$

Substituting into Wave equation  $\gamma[-V_0^+ e^{-\gamma z} + V_0^- e^{\gamma z}] = (R + j\omega L)I(z)$  yields:

$$I(z) = \frac{\gamma}{(R + j\omega L)} [V_0^+ e^{-\gamma z} - V_0^- e^{\gamma z}] \quad (28)$$

$Z_0$  is the ratio of  $V/I$  for forward and backward waves and not the ratio of  $V/I$  for the total wave:

$$Z_0 = V_0^+/I_0^+ = V_0^-/I_0^- = (R + j\omega L)/\gamma = \sqrt{(R + j\omega L)/(G + j\omega C)}$$

Wave nature of the TL leads to the following consequences:

- Bi-directionality: Wave propagation is occurring both ways (incident and reflected)
- Load: A TL is said to be perfectly terminated if  $Z_0$  is used as a load impedance preventing undesired reflections back to the source feeding the TL causing return loss.
- Skin effect: When frequency increases currents get closer to the surface increasing resistance and loss.
- Echoes: Reflections at the junction of two different lines due to impedance mismatch or at the termination load, line imperfections...
- Symmetry: Joining a cable carrying a symmetric signal (like Audio) and another carrying an asymmetric signal (like Video) requires a device called balun (porte-manteau word for balanced/unbalanced).
- Interference: TL are prone to EMI (Electro-Magnetic Interference) and thus should be protected by special anti-EMI filters (like ferrite core rings used to protect Computer cables). In contrast Optical fibers are free of EMI.
- Ground: Neighboring TL should have a well defined ground otherwise EMI occurs among them. Coaxial Cable TV companies had to deal with ground differing between neighboring buildings leading to noisy TV reception. In contrast, Optical fibers are free of ground definition.
- Cross-talk (XT) [10] originating from internal reflections with a TL may cause impairments as in telephone lines where there are NEXT [10](Near End XT) and FEXT [10] (Far End XT)
- Wire gauge: This sizing parameter impacts all properties above

For a perfectly terminated TL with length  $d$ , the transfer function at frequency  $f$  is given by [10]:

$$H(f, d) = \left[ \frac{I(z=d)}{I(z=0)} \right]_+ = \left[ \frac{V(z=d)}{V(z=0)} \right]_+ = \exp(-\gamma d).$$

### C. Gauge

The series resistance for long cables is often specified in  $\Omega/[1000 \text{ feet}]$  (about  $\Omega/[305 \text{ m}]$ ). In any signal loss evaluation the resistance of both outgoing and return pathways should be added, since current flows equally in both, and both dissipate power.

There are eight rules of thumb for estimating the DC resistance of round copper wires:

1. The American Wire Gauge (AWG) system is a logarithmic measure of the diameter of round wires. The larger the gauge, the smaller the wire.
2. Six AWG points halves the diameter.
3. Area being proportional to diameter-squared, three AWG points halves the cross-sectional area.
4. Three AWG points doubles the wire resistance. The resistance per unit length  $\Omega/[1000 \text{ feet}]$  is related to AWG in dB with a 10-AWG wire having  $1 \Omega/[1000 \text{ feet}]$ . Therefore, every increase of 3 AWG ( $\approx 10 \times \log_{10}(2)$ ) increases the resistance per unit length by a factor of two. Thus 13-AWG wire has  $2 \Omega/[1000 \text{ feet}]$ , 16-AWG wire has  $4 \Omega/[1000 \text{ feet}]$ ...
5. A round conductor of size such as 24-AWG has a nominal diameter of 0.507 mm (0.02 in.) and a resistance at room temperature of  $0.085 \Omega/\text{m}$  ( $\sim 26 \Omega/[1000 \text{ feet}]$ ).
6. Twisted-pair 24-AWG cable has a total series resistance (adding both wires in series) of  $0.170 \Omega/\text{m}$  ( $\sim 52 \Omega/[1000 \text{ feet}]$ ) at room temperature.
7. RG-58/U coaxial cable using a stranded core of 20-AWG has a resistance at room temperature of  $0.034 \Omega/\text{m}$  ( $10.3 \Omega/[1000 \text{ feet}]$ ).
8. The resistance of copper increases 0.39% with every Celsius degree increase in temperature. Over a  $70^\circ\text{C}$  temperature range, that amounts to a variation of 31%.

The general formula for the wire gauge given the resistance  $R$  in  $\Omega/[1000 \text{ feet}]$  is

$$AWG = 10 \log_{10} R + 10, \quad R = 10^{\frac{AWG-10}{10}} \Omega/[1000 \text{ feet}]. \quad (29)$$

A wire of length  $\ell$ , cross-sectional area  $A$  and conductivity  $\sigma$  has resistance  $\ell/\sigma A$ , or resistance per unit length  $R = 1/\sigma A$ . Using formula above gives:

$$A \propto 10^{\frac{AWG-10}{10}} \quad \text{yielding} \quad D \propto 10^{\frac{AWG-10}{10}} \quad (30)$$

where  $D$  is the wire diameter.

Conventionally a 10 AWG wire has a diameter of 0.10 inches (1 inch= 2.54 cm) giving:

$$D = 10^{-\frac{AWG+10}{10}} \quad (31)$$

Thus a wire gauge is related to diameter via:

$$AWG = -20 \log_{10} D - 10. \quad (32)$$

A rule of thumb for wire sizing is that a 700 circular mils cross-sectional area per ampere to avoid undue temperature rise in the wire. If some temperature rise could be tolerated in the wire then a different number would apply.

The awkward definition of a circular area measured in circular mils (a mil is 0.001 inch) originates from imposing the area of the square whose side has the same length as the diameter of the circle, i.e. just the diameter squared.

The current carrying capacity in amps is therefore (with  $D$  measured in inches)

$$I = \frac{1}{700} 10^6 \times D^2 \quad (33)$$

or in terms of AWG

$$I = \frac{1}{700} 10^{\frac{50-AWG}{10}} \quad (34)$$

solving for AWG in terms of current

$$AWG = 50 - 10 \log_{10}(700 I) \quad (35)$$

Substitution of  $R$  and  $I$  from formulas above yields the power  $P = RI^2$  dissipated per foot (or 30.48 cm) of wire as:

$$P = \left(\frac{1}{700}\right)^2 10^{\frac{50-AWG}{10}} \text{Watts}/[1000 \text{ feet}] \quad (36)$$

#### D. EMI filtering

Suppression of EMI with ring cores is based on ferrite properties. Ferrites are a class of ceramic ferromagnetic materials that by definition can be magnetized to produce large magnetic flux densities in response to small applied magnetic fields. They are magnetic insulators, first used as replacements for laminated and slug iron core materials in low loss inductors intended for use above 100 kHz. At these frequencies, laminated and slug iron are impacted by excessive eddy current losses whereas the high volume resistivity of ferrite cores limit power loss to a fraction of other core materials.

Ferrites intended for EMI applications above 30 MHz are mixtures of iron, nickel and zinc oxides that are characterized by high volume resistivity ( $10^5 \Omega \cdot \text{m}$ ) and moderate initial permeability (100 to 1500). Ferrites are most frequently used as two terminal circuit elements, or in groups of two terminal elements. High frequency noise suppression performance of ferrites can be traced back to their frequency dependent complex impedance, as shown in Fig. 7.

The impedance  $Z(f) = j\omega L(f)$  versus frequency  $f$  ( $\omega = 2\pi f$ ) where  $L(f) = \mu_r(f) \cdot L_0$  is a frequency dependent inductance and  $\mu_r(f)$  is a complex relative permeability with  $L_0$  a reference inductance. This originates from the above observation (cf. section II E) that the inductance of e.g. a wire  $L = n_t \mu \ell F(\ell/d)$  [11] indicating that  $L$  is proportional to the permeability [8], the number of turns  $n_t$  and some function  $F$  depending on wire geometrical factors  $\ell, d$ .

Writing  $\mu_r(f) = \mu_r'(f) - j\mu_r''(f)$  yields:

$$Z(f) = j\omega \cdot (\mu_r'(f) - j\mu_r''(f)) \cdot L_0 = \omega \cdot \mu_r''(f) \cdot L_0 + j\omega \cdot \mu_r'(f) \cdot L_0, \quad (37)$$

The impedance  $Z(f) = R(f) + jX_L(f)$  with  $R(f) = \omega \cdot \mu_r''(f) \cdot L_0$  and the inductive reactance  $X_L(f) = \omega \cdot \mu_r'(f) \cdot L_0$ .

Then  $|Z(f)| = \sqrt{R^2(f) + X_L^2(f)} = \omega \cdot L_0 \cdot \sqrt{[\mu_r'(f)]^2 + [\mu_r''(f)]^2}$ .

At low frequencies (below 10 MHz), the impedance has a small, inductive impedance of less than 100  $\Omega$  (cf. Fig. 7). At higher frequencies, the impedance increases to 600  $\Omega$ , and becomes essentially resistive above 100 MHz (cf. Fig. 7). When used as EMI filters, ferrites can thus provide resistive loss to attenuate and dissipate (with small quantities of heat) high frequency noise while presenting negligible series impedance to lower frequency signal values.

When properly selected and implemented, ferrites can thus provide significant EMI reduction while remaining transparent to normal circuit operation. For high frequency applications, ferrites behave as frequency dependent resistors.

#### E. Joining cables of different symmetries: Balun transformer

The first step to connect cables of different symmetries such as a coaxial cable (asymmetric) and a twisted pair (symmetric) is to build a pulse transformer [13].

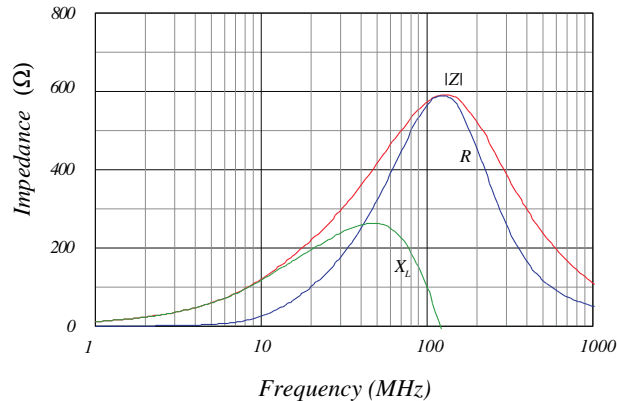


**Fig.7:** Typical behavior of  $|Z|$ ,  $R$ ,  $X_L$  versus frequency for a ring core ferrite such as MnZn or NiZn. Adapted from ref. [12]

A simple inverting pulse transformer consists of a coaxial cable wound on a ferrite toroid [13]. At one end of the coax, the outer sheath is grounded and the inner conductor is connected to the pulse source. At the other end of the coax, due to the large inductance of the winding, which is common to both inner and outer conductors, the connections may be reversed. The inner conductor may be grounded while the outer conductor used as the pulse source, is identical to the input pulse but of opposite sign [13].

In order to make a balun transformer, two inverting transformers have their inputs connected in parallel on one side and in series on the other.

For example, 100  $\Omega$  coaxial cable could be used to provide a 50  $\Omega$  to 200  $\Omega$  balun transformer of this kind. Using 100  $\Omega$  twisted pair, or balanced line, would be even better. This method of constructing a balun may have been first described by Talkin and Cuneo [14].

Another balun transformer described in ref. [13] uses four inverting transformers, based on four 50  $\Omega$  TP of equal length wound on four ferrite ring cores. In practice, 500 mm of TP is used on each 25 mm diameter core made of a high frequency, high permeability ferrite (such as MnZn or NiZn).

A 50  $\Omega$  twisted pair (usually 100  $\Omega$ ) is easily made from two 0.4 mm polyurethane coated wires, twisted to a 5 mm pitch. Four 50  $\Omega$  lines are connected in series/parallel on the 50  $\Omega$  side, to give a 50  $\Omega$  input impedance, while all four are connected in series, on the output side, to give the 200  $\Omega$  balanced output. This configuration has a very great advantage over the simpler one, using just two 100  $\Omega$  lines, in that the balun described in ref. [13] is an isolating transformer: there is no d.c. path between input and output.

A more expensive way of making the same balun, with better very high frequency performance, is to use four miniature 50  $\Omega$  coaxial cables, instead of the TP, and ferrite ring cores around each cable. This gives a linear layout to the balun and reduces the shunt capacitance.

## IV. TRANSMISSION LINE IN TELECOMMUNICATIONS

### A. Transfer function $H(f, d)$ versus communication distance

In telecommunications, one deals with signal propagation over some communication distance [15] as displayed in Fig. 8. This means attenuation and delay with distance implying the use of repeaters in order to amplify and reshape the signal as illustrated in Table 1.

The space dependent  $h(t, d)$  displayed in Fig. 8 can be Fourier transformed to become the TL transfer function is given in general by  $H(f, d) = \mathcal{F}[h(t, d)]$ .

In the TL case  $H(f, d) = \exp(-\gamma d)$  where  $\gamma = \sqrt{(R + j\omega L)(G + j\omega C)}$  and  $\omega = 2\pi f$ .

Fig. 9 and Fig. 10 show that  $|H(f, d)|$  gets narrower versus frequency and its amplitude decreases with distance. These losses are due to the combined actions of skin effect and exponential amplitude attenuation.

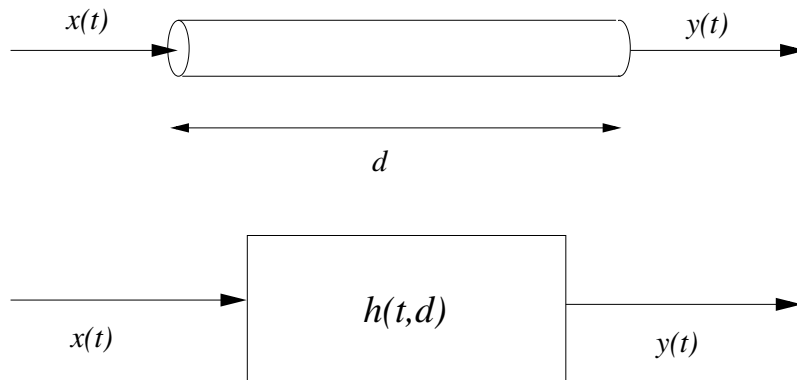


**Fig.8:** Similarly to a signal  $x(t)$  entering a device and emerging from it as  $y(t)$ , one might draw analogy with an impulse response depending on traveling distance  $d$  across a channel represented by a transmission line containing wires, coaxial cables...

| Transmission media  | Frequency Range | Typical Attenuation | Typical Delay | Repeater Spacing |
|---------------------|-----------------|---------------------|---------------|------------------|
| TP (with loads)     | 0 to 3.5 kHz    | 0.2 dB/km @ 1 kHz   | 50 $\mu$ s/km | 2 km             |
| Trunk of bundled TP | 0 to 1 MHz      | 0.7 dB/km @ 1 kHz   | 5 $\mu$ s/km  | 2 km             |
| Coaxial cable       | 0 to 500 MHz    | 7 dB/km @ 10 MHz    | 4 $\mu$ s/km  | 1 to 9 km        |
| Optical fiber       | 186 to 370 THz  | 0.2 to 0.5 dB/km    | 5 $\mu$ s/km  | 40 km            |

**Table 1:** Transmission characteristics of several communication channels beginning in kHz with TP and ending in THz (Tera Hertz or  $10^{12}$  Hz) with optical fibers. Trunks containing 25 or 50 bundled TP are used in North America communication networks. Adapted from Stallings [16].

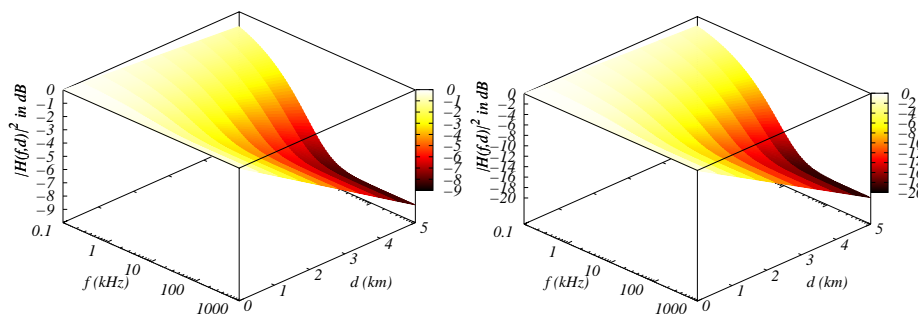


**Fig.9:** (Color on-line) (left) 3D Transfer function  $|H(f,d)|$  for a low-loss gauge 19 wire. (right) 3D Transfer function  $|H(f,d)|$  for a gauge 22 wire. Note that  $|H(f,d)|$  scale is logarithmic (in dB) as well as the frequency that is limited to 1 MHz.

## B. Crosstalk

Crosstalk (XT) noise arises because many twisted pairs are bundled together into a single cable. Electromagnetic coupling between one pair and its neighboring pairs in a bundle generate crosstalk EMI. Each copper pair is twisted in order to reduce the effects of XT and the manufacture of these twisted pairs is tightly controlled to maintain balance between two wires in a pair. In North-America TP are bundled in a 50 pair group twisted with different pitches to further reduce the coupling between pairs at higher frequencies [10]. In Europe TP are bundled in quads containing four pairs with typically two spatial arrangements as displayed in Fig. 11.

This type is mainly used in some European countries and Japan. A quad consists of two pairs twisted together, forming the smallest unit. There exist two forms of quads as shown in Fig. 11, the star-quad being widely used. XT characteristics of quad cables are significantly different from the ones of twisted pair cables. In quad cables, typically 5 quads form a binder group and 5 such groups are twisted together to form a bundle. Therefore a bundle contains

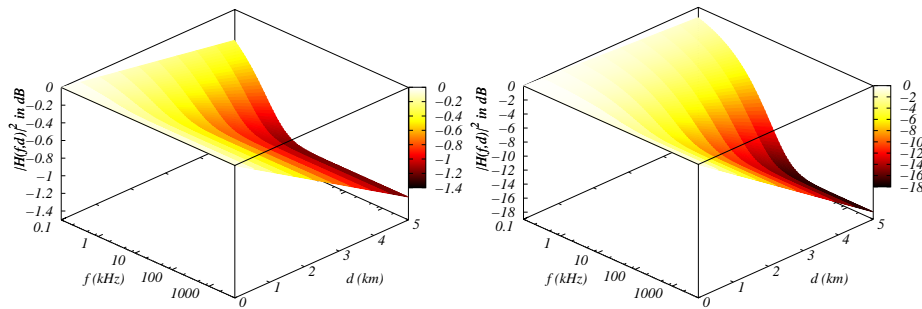


**Fig.10:** (Color on-line) (left) 3D Transfer function  $|H(f, d)|$  for a low-loss Coaxial cable. (right) 3D Transfer function  $|H(f, d)|$  for an RG58 Coaxial cable. Both cables have  $Z_0 = 50\Omega$ . Note that  $|H(f, d)|$  scale is logarithmic (in dB) as well as the frequency that is limited to 5 MHz.

25 quads, equivalent to 50 pairs.

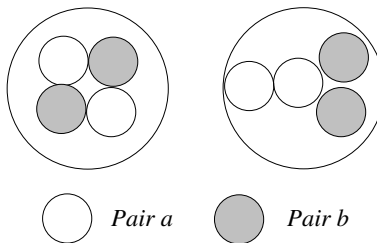


**Fig.11:** European Cable made of a bundle of four TP organized geometrically in two patterns in order to combat EMI. (left) Star quad, (right) Dieselhorst-Martin quad

There are two main forms of XT interference: Near End crosstalk (NEXT) and Far End crosstalk (FEXT) as illustrated in Figure 12, NEXT is the result of EMI on the same end of the cable whereas FEXT is at the opposite end of the cable.

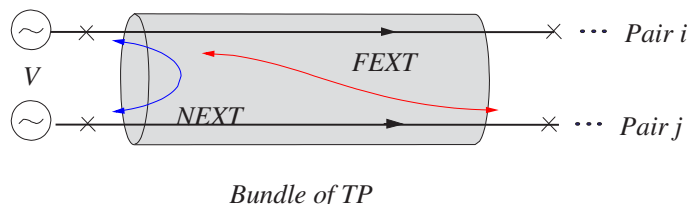


**Fig.12:** Cable made of a bundle of TP illustrating NEXT and FEXT interference originating from EMI between two arbitrary pairs.

In bundled TP networking environments, NEXT interference is more important than FEXT because of the weaker attenuation that FEXT encounters while traveling down the line [10].

NEXT coupling has a length  $d$  dependent transfer function  $H_n$  such that [10]:

$$|H_n(f, d)|^2 = \chi_n f^{\frac{3}{2}} \quad (38)$$

where  $f$  is frequency,  $d$  is cable length, and  $\chi_n$  is a coupling factor that depends on cable characteristics. The value for  $\chi_n$  is given as [17]  $10^{-9}/[kHz]^{\frac{3}{2}}$ .

When a data signal is received, it is attenuated however, it must have a greater magnitude than NEXT noise in order for the signal to be properly decoded. NEXT noise from eq. 38 is plotted on the same graph as the gain characteristics of e.g. 24 gauge wire in order to compare NEXT noise to the attenuated signal that must be significantly larger than noise. Noise margin is usually of the order of 10 dB.

FEXT coupling has a length  $d$  dependent transfer function  $H_{f,d}$  such that [10, 17]:

$$|H_f(f, d)|^2 = \chi_f f^2 d \quad (39)$$

where  $\chi_f$  is a coupling factor about [17]  $3.36 \times 10^{-12}/[km.(kHz)^2]$ .

Fig. 13 displays frequency variation of a 24 gauge TP transfer function  $|H(f, d)|^2$ , along with NEXT and FEXT. NEXT cuts  $|H(f, d)|^2$  at a high frequency ( $\sim 20$  MHz) whereas FEXT is smaller than NEXT at low frequency and becomes comparable to NEXT at very high frequency ( $> 100$  MHz).

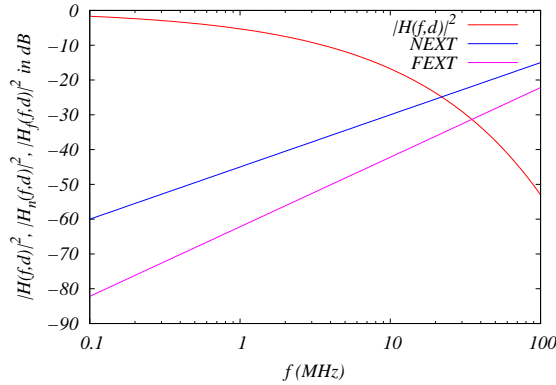


**Fig.13:** Frequency variation of a 24 gauge TP transfer function  $|H(f, d)|^2$ , along with NEXT and FEXT. NEXT is given by  $|H_n(f, d)|^2 = \chi_n f^{\frac{3}{2}}$  with  $\chi_n = 10^{-9}/[kHz]^{\frac{3}{2}}$ . FEXT is given by  $|H_f(f, d)|^2 = \chi_f f^2 d$  with  $\chi_f = 3.36 \times 10^{-12}/[km.(kHz)^2]$ . Cable length  $d = 180$  m and its characteristics are given in Table 3. Note that FEXT is smaller than NEXT at low frequency and becomes comparable to NEXT at high frequency. Adapted from Kalet *et al.* [17].

### C. Cable Termination

Checking a cable for reflection by its terminating end is done by sending pulses in the cable and looking at the echoes (no echoes exist in a well-terminated cable), thus it is possible to check if anything is wrong with the joints, loads or terminators and repair or replace the cable since an echo is an interference to the signal.

A time domain reflectometer (TDR) performs several tasks, such as:

- Sending a well-defined voltage pulse down the line and waiting for the echo by displaying the pulse and echo on an oscilloscope screen.
- Measuring echo time to find cable length or distance to some impurity, defect, corrosion, crack...

As an example, a USB-1 cable termination requirement is such that a  $[0:3.6V]$  signal traveling into a  $51.75 \Omega$  line with a  $28 \Omega$  termination voltage swings between 4.6 and -1.0 V.

It is recommended to size the series termination resistors to make a  $44 \Omega$  termination. This does bring the terminations well within the standard  $\pm 15\%$  impedance tolerance.

Another example is the nominal cable impedance for Firewire-a is  $110 \Omega$ , which is a typical number for a high speed TP. Cable quality is an important issue for all high speed serial transmission schemes, and Firewire-a is no exception with speeds up to Gigabits/s. The nominal termination impedance is  $112 \Omega$ .

**Note:** Length limitation of cables provides a way to avoid terminators as for instance 4.5 m for Firewire-a and 5 m for USB-1 [16].

### D. Secure communications

The principle of secure (spread-spectrum) digital communications is based on multiplying the message (made of 0 and 1) by a PRBS. Crypting the message amounts to modify the signal carrying it in a way such that it looks like

noise [15].

As explained in section II A 1 PRBS are produced in a controlled fashion with a deterministic algorithm akin to pseudo-random numbers used in a Monte-Carlo algorithm or some other type of simulation [5].

The main goal of PRBS generation, is to draw 0 or 1 in an equally probable fashion in order to have highly efficient crypting of the message (largest bandwidth or spreading).

The PRBS sequence  $a[n]$  is produced with a shift register XOR operation as illustrated in fig. 14.

A particularly efficient method for producing PRBS is based on primitive polynomials modulo 2 or Galois polynomials [18] with the following arithmetic:

$$0 \oplus 0 = 0, 0 \oplus 1 = 1, 1 \oplus 0 = 1, 1 \oplus 1 = 0 \quad (40)$$

$\oplus$  is the usual symbol for modulo 2 arithmetic corresponding to the logical XOR operation that may be done with shift registers [5].

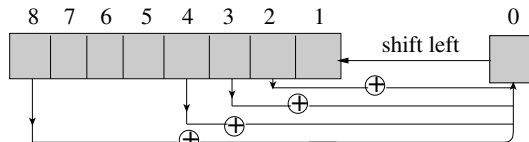


**Fig.14:** Shift register connections with feedback set up for PRBS [5] generation on the basis of a (modulo 2) primitive polynomial given by  $1 + x^2 + x^3 + x^4 + x^8$ . It is of order 8 and tap connections (8,4,3,2,0) are shown (cf. Table 2).

The method for producing PRBS illustrated in fig. 14 requires only a single shift register  $n$  bits long and a few XOR or mod 2 bit addition operations ( $\oplus$  gates).

The terms that are allowed to be XOR summed together are indicated by shift register taps. There is precisely one term for each nonzero coefficient in the primitive polynomial except the constant (zero bit) term.

The coefficients of primitive polynomials modulo 2 are zero or one e.g.  $x^4 + x^3 + 1$ , moreover they cannot be decomposed into a product of simpler modulo 2 polynomials. An illustrative example is  $x^2 + 1$  that cannot be decomposed into simpler polynomials with real coefficients but can be decomposed into polynomials with complex coefficients  $x^2 + 1 = (x + j)(x - j)$  with  $j = \sqrt{-1}$ . When this polynomial is viewed as a Galois polynomial, it is not primitive since it can be decomposed into a product of simpler polynomials  $x^2 + 1 \equiv x^2 + 2x + 1 = (x + 1)(x + 1)$  since in modulo 2 arithmetic the term  $2x$  is equivalent to 0 according to the above arithmetic rule ( $1 \oplus 1 = 0$ ).

Table 2 contains a list of polynomials for  $n \leq 10$ , showing that for a primitive polynomial of degree  $n$ , the first and last term are 1.

In order to decode the PRBS crypted message a correlation operation based on the  $x[n]$  auto-correlation is given by:

$$R_{xx}[k] = \frac{1}{N-1} \sum_{i=0}^{N-2} x[i]x[k+i] \quad (41)$$

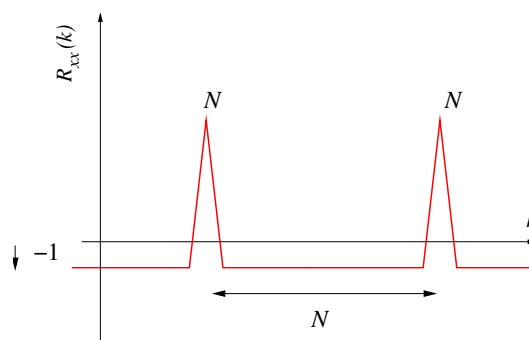


**Fig.15:** Property of PRBS auto-correlation  $R_{xx}$  showing peaks that enables decoding the message and displaying largest length  $N = 2^n - 1$  with  $n$  the number of coding bits. It is remarkable that peak values  $N = 2^n - 1$  are distant by period of same value  $N = 2^n - 1$ .

Since  $x[k] = (-1)^{a[k]}$  with  $a[k] = 0$  or  $1$  yields  $x[k] = +1$  or  $-1$  with  $+1/-1$  equally probable, we obtain:

$$R_{xx}[k] = \frac{1}{N-1} \sum_{i=0}^{N-2} (-1)^{(a[i] \oplus a[k+i])} \quad (42)$$

with  $N = 2^n - 1$  where  $n$  is the number of coding bits or PRBS order.  $N$  is the period or the length of the PRBS with the same value as the peak value (cf. Fig. II A 1).

As a result, the auto-correlation  $R_{xx}$  displays a Dirac  $\delta$  function-like behavior as observed in Fig. 15 required for message decoding.

| Connection Nodes | Equivalent Polynomial       |
|------------------|-----------------------------|
| (1, 0)           | $1 + x$                     |
| (2, 1, 0)        | $1 + x + x^2$               |
| (3, 1, 0)        | $1 + x + x^3$               |
| (4, 1, 0)        | $1 + x + x^4$               |
| (5, 2, 0)        | $1 + x^2 + x^5$             |
| (6, 1, 0)        | $1 + x + x^6$               |
| (7, 1, 0)        | $1 + x + x^7$               |
| (8, 4, 3, 2, 0)  | $1 + x^2 + x^3 + x^4 + x^8$ |
| (9, 4, 0)        | $1 + x^4 + x^9$             |
| (10, 3, 0)       | $1 + x^3 + x^{10}$          |

**Table 2:** List of the first 10 Galois polynomials. Adapted from Ref. [5]

#### APPENDIX A: CABLE PRIMARY CONSTANTS

| $f$<br>(kHz) | $R$<br>( $\Omega$ /mile) | $L$<br>(mH/mile) | $G$<br>( $\mu\Omega^{-1}$ /mile) | $C$<br>( $\mu\text{F}$ /mile) | Complex $Z_0$<br>( $\Omega, \Omega$ ) | $\gamma$<br>(dB/mile) | $\gamma$<br>(%/mile) |
|--------------|--------------------------|------------------|----------------------------------|-------------------------------|---------------------------------------|-----------------------|----------------------|
| 1            | 277.2                    | 0.986            | 0.115                            | 0.083                         | (521,-510)                            | 2.310                 | 15.6                 |
| 5            | 277.5                    | 0.984            | 0.466                            | 0.083                         | (244,-218)                            | 4.942                 | 35.4                 |
| 10           | 278.0                    | 0.982            | 0.853                            | 0.083                         | (182,-146)                            | 6.625                 | 54.4                 |
| 50           | 286.0                    | 0.984            | 3.458                            | 0.083                         | (117,-47)                             | 10.628                | 175.1                |
| 100          | 308.4                    | 0.935            | 6.320                            | 0.083                         | (109,-27)                             | 12.235                | 327.2                |
| 150          | 337.2                    | 0.920            | 8.993                            | 0.083                         | (107,-20)                             | 13.665                | 480.5                |
| 300          | 431.6                    | 0.888            | 16.440                           | 0.083                         | (104,-13)                             | 17.975                | 935                  |
| 500          | 541.7                    | 0.857            | 25.633                           | 0.083                         | (102,-10)                             | 23.048                | 1526                 |

**Table 3:** 24 gauge Pulp Insulated Cables (PIC) primary constants at 20°C. 1 mile= 1.6 km. Adapted from Werner [10].

| Wire Pairs   | $f$     | $R$<br>( $\Omega/\text{km}$ ) | $L$<br>(mH/km) | $C$<br>( $\mu\text{F}/\text{km}$ ) | $\alpha$<br>(dB/km) | $Z_0$<br>( $\Omega/\text{km}, ^\circ/\text{km}$ ) |
|--|---------|-------------------------------|----------------|------------------------------------|---------------------|---|
| 22 AWG wire  | 100 Hz  | 107                           | 0.60           | 0.05                               | 0.36*               | 1850,-45 $^\circ$ *                               |
|  | 10 kHz  |                               | 0.60           | 0.05                               | 3.0*                | 190,-35 $^\circ$ *                                |
|  | 100 kHz |                               | 0.60           | 0.05                               | 4.2*                | 110,-8 $^\circ$ *                                 |
| 19 AWG toll pair,<br>no loading coils  | 100 Hz  | 52                            | 0.68           | 0.04                               | 0.21                | 1440,-45 $^\circ$ *                               |
|  | 10 kHz  | 52                            | 0.68           | 0.04                               | 1.5                 | 160,-25 $^\circ$ *                                |
|  | 100 kHz | 85                            | 0.68           | 0.04                               | 3.0                 | 130,-6 $^\circ$ *                                 |
| Copper wire pair,<br>spaced 20.3 cm,<br>33 insulators/km,<br>wire diameter: 2.6 mm | 100 Hz  | 6.4                           | 2.1            | 0.0055                             | 0.026               | 1380,-39 $^\circ$ *                               |
|  | 10 kHz  | 8.0                           | 2.1            | 0.0055                             | 0.058               | 620,-2 $^\circ$ *                                 |
|  | 100 kHz | 22                            | 2.1            | 0.0055                             | 0.16                | 620,-0.5 $^\circ$ *                               |

**Table 4:** Measured characteristics of selected wires made from polyethylene dielectric; the inner conductor is a stranded bundle. AWG is American Wire Gauge. An asterisk (\*) denotes a value calculated via  $Z_0 = \sqrt{(R + j\omega L)/(G + j\omega C)}$ ,  $\omega = 2\pi f$ .  $\alpha = Re(\gamma)$  is amplitude attenuation. Adapted from Anderson [19].

| Coaxial Cables     | Diameter (mm)   |            | $C$<br>(pF/m) | $\alpha$<br>(dB/100 m) | $Z_0$<br>( $\Omega$ , real) |
|--------------------|-----------------|------------|---------------|------------------------|-----------------------------|
|                    | Inner Conductor | Dielectric |               |                        |                             |
| RG-58 C/U          | 0.9             | 2.9        | 94            | 4.6                    | 50                          |
| RG-213U, RG-8A/U   | 2.3             | 7.2        | 96            | 2.2                    | 50                          |
| RG-11A/U, RG-12A/U | 1.2             | 7.2        | 67            | 2.2                    | 75                          |

**Table 5:** Measured Characteristics of Selected Coaxial Cables. RG is Radio Guide.  $\alpha = Re(\gamma)$  is amplitude attenuation. Cable measurements are performed at 10 MHz. Adapted from Anderson [19].

| Designation | Cable nature                 | Main Application                    | $R$                | $L$                     | $G$                             | $C$                   | $Z_0$    |
|-------------|------------------------------|-------------------------------------|--------------------|-------------------------|---------------------------------|-----------------------|----------|
|             |                              |                                     | $\Omega/\text{km}$ | $\mu\text{H}/\text{km}$ | $\text{n}\Omega^{-1}/\text{km}$ | $\text{nF}/\text{km}$ | $\Omega$ |
| CAT5        | TP                           | Data transmission                   | 176                | 490                     | $< 2$                           | 49                    | 100      |
| CAT5e       | TP                           | Data transmission                   | 176                |                         | $< 2$                           |                       | 100      |
| CW1308      | TP                           | Telephony                           | 98                 |                         | $< 20$                          |                       |          |
| Low loss    | Coaxial<br>(foam dielectric) | Radio frequency<br>transmitter feed | 2.86               | 188                     |                                 | 75                    | 50       |
| RG58        | Coaxial                      | Radio frequency                     | 48                 | 253                     | $< 0.01$                        | 101                   | 50       |
| RG59        | Coaxial                      | Video                               | 36                 | 430                     |                                 | 69                    | 75       |
| RG59        | Coaxial<br>(foam dielectric) | Video                               | 20.4               | 303                     |                                 | 54                    | 75       |

**Table 6:** Measured Characteristics of Selected Cables. RG is Radio Guide. CAT is Category. CW is Continuous Wave. Adapted from Anderson [19].

## APPENDIX B: LAPLACE TRANSFORM OF TYPICAL SIGNALS

- $\delta(t)$ ,  $\delta(t - \tau)$

$$\mathcal{L}[\delta(t)] = \int_{-\infty}^{\infty} \delta(t)e^{-st} dt = e^0 = 1, \quad \forall s$$

Moreover, due to time shifting property [3], we have

$$\mathcal{L}[\delta(t - \tau)] = e^{-s\tau}, \quad \forall s$$

- $u(t)$ ,  $t u(t)$ ,  $t^n u(t)$

Due to the property of time domain integration, we have

$$\mathcal{L}[u(t)] = \mathcal{L}\left[\int_{-\infty}^t \delta(\tau) d\tau\right] = \frac{1}{s}, \quad \text{Re}[s] > 0$$

Applying the s-domain differentiation property to the above, we have

$$\mathcal{L}[tu(t)] = -\frac{d}{ds}\left[\frac{1}{s}\right] = \frac{1}{s^2}, \quad \text{Re}[s] > 0$$

and in general

$$\mathcal{L}[t^n u(t)] = \frac{n!}{s^{n+1}}, \quad \text{Re}[s] > 0$$

- $e^{-at}u(t)$ ,  $te^{-at}u(t)$

Applying the s-domain shifting property to

$$\mathcal{L}[u(t)] = \frac{1}{s}, \quad \text{Re}[s] > 0$$

we have

$$\mathcal{L}[e^{-at}u(t)] = \frac{1}{s+a}, \quad \text{Re}[s] > -a$$

Applying the same property to

$$\mathcal{L}[t^n u(t)] = \frac{n!}{s^{n+1}}, \quad \text{Re}[s] > 0$$

we have

$$\mathcal{L}[t^n e^{-at}u(t)] = \frac{n!}{(s+a)^{n+1}}, \quad \text{Re}[s] > -a$$

- $e^{-j\omega_0 t}u(t)$ ,  $\sin(\omega_0 t)u(t)$ ,  $\cos(\omega_0 t)u(t)$

Letting  $a = \pm j\omega_0$  in

$$\mathcal{L}[e^{-at}u(t)] = \frac{1}{s+a}, \quad \text{Re}[s] > -\text{Re}[a]$$

we get

$$\mathcal{L}[e^{-j\omega_0 t}u(t)] = \frac{1}{s+j\omega_0} \quad \text{and} \quad \mathcal{L}[e^{j\omega_0 t}u(t)] = \frac{1}{s-j\omega_0} \quad \text{Re}[s] > 0$$

and therefore

$$\mathcal{L}[\cos(\omega_0 t)u(t)] = \frac{1}{2}\mathcal{L}[e^{j\omega_0 t} + e^{-j\omega_0 t}] = \frac{1}{2}\left[\frac{1}{s-j\omega_0} + \frac{1}{s+j\omega_0}\right] = \frac{s}{s^2 + \omega_0^2}$$

and

$$\mathcal{L}[\sin(\omega_0 t)u(t)] = \frac{1}{2j}\mathcal{L}[e^{j\omega_0 t} - e^{-j\omega_0 t}] = \frac{1}{2j}\left[\frac{1}{s-j\omega_0} - \frac{1}{s+j\omega_0}\right] = \frac{\omega_0}{s^2 + \omega_0^2}$$

- $t \cos(\omega_0 t)u(t)$ ,  $t \sin(\omega_0 t)u(t)$

Letting  $a = \pm j\omega_0$  in

$$\mathcal{L}[te^{-at}u(t)] = \frac{1}{(s+a)^2}, \quad \text{Re}[s] > -a$$

we get

$$\mathcal{L}[te^{-j\omega_0 t}u(t)] = \frac{1}{(s + j\omega_0)^2}, \quad \text{and} \quad \mathcal{L}[te^{j\omega_0 t}u(t)] = \frac{1}{(s - j\omega_0)^2}, \quad \text{Re}[s] > -a$$

Furthermore we have

$$\mathcal{L}[t \cos(\omega_0 t)u(t)] = \frac{1}{2}\mathcal{L}[t(e^{j\omega_0 t} + e^{-j\omega_0 t})] = \frac{1}{2}\left[\frac{1}{(s - j\omega_0)^2} + \frac{1}{(s + j\omega_0)^2}\right] = \frac{s^2 - \omega_0^2}{(s^2 + \omega_0^2)^2}$$

and

$$\mathcal{L}[t \sin(\omega_0 t)u(t)] = \frac{1}{2j}\mathcal{L}[t(e^{j\omega_0 t} - e^{-j\omega_0 t})] = \frac{1}{2j}\left[\frac{1}{(s - j\omega_0)^2} - \frac{1}{(s + j\omega_0)^2}\right] = \frac{2s\omega_0}{(s^2 + \omega_0^2)^2}$$

- $e^{-at} \cos(\omega_0 t)u(t)$ ,  $e^{-at} \sin(\omega_0 t)u(t)$

Applying s-domain shifting property to:

$$\mathcal{L}[\cos(\omega_0 t)u(t)] = \frac{s}{s^2 + \omega_0^2}, \quad \mathcal{L}[\sin(\omega_0 t)u(t)] = \frac{\omega_0}{s^2 + \omega_0^2} \quad (\text{B1})$$

we get, respectively

$$\mathcal{L}[e^{-at} \cos(\omega_0 t)u(t)] = \frac{s + a}{(s + a)^2 + \omega_0^2}, \quad \mathcal{L}[e^{-at} \sin(\omega_0 t)u(t)] = \frac{\omega_0}{(s + a)^2 + \omega_0^2} \quad (\text{B2})$$

## APPENDIX C: FOURIER TRANSFORM OF TYPICAL SIGNALS

- **Unit impulse**

Due to the property of time derivative [3]

$$\text{If } \mathcal{F}[x(t)] = X(\omega), \quad \text{then } \mathcal{F}\left[\frac{d}{dt}x(t)\right] = j\omega X(\omega)$$

we can get the Fourier transform of a unit impulse as the time derivative of a unit step function:

$$\mathcal{F}[\delta(t)] = \mathcal{F}\left[\frac{d}{dt}u(t)\right] = j\omega \mathcal{F}[u(t)] = j\omega \frac{1}{j\omega} = 1$$

Alternatively, by definition, the forward Fourier transform of an impulse function  $\delta(t)$  is

$$\Delta(\omega) = \mathcal{F}[\delta(t)] = \int_{-\infty}^{\infty} \delta(t)e^{-j\omega t} dt = e^{-j\omega 0} = 1$$

and the inverse transform is

$$\frac{1}{2\pi} \int_{-\infty}^{\infty} \Delta(\omega)e^{j\omega t} d\omega = \frac{1}{2\pi} \int_{-\infty}^{\infty} e^{j\omega t} d\omega = \delta(t)$$

- **Unit step**

Unit step function is defined as

$$u(t) = \begin{cases} 1 & t \geq 0 \\ 0 & t < 0 \end{cases}$$

and its Fourier transform is

$$U(\omega) = \mathcal{F}[u(t)] = \int_{-\infty}^{\infty} u(t)e^{-j\omega t} dt = \int_0^{\infty} e^{-j\omega t} dt$$

This integral does not converge. But if we first consider the Fourier transform of one-sided exponential decay

$$\mathcal{F}[e^{-at}u(t)] = \frac{1}{a + j\omega}$$

and let  $a = 0$ , we have

$$\mathcal{F}[u(t)] = \frac{1}{j\omega}$$

- **Exponential decay**

$$x(t) = e^{-at}u(t) \quad (a > 0)$$

$$\begin{aligned} \mathcal{F}[e^{-at}u(t)] &= \int_{-\infty}^{\infty} x(t)e^{-j\omega t} dt = \int_0^{\infty} e^{-at}e^{-j\omega t} dt \\ &= \frac{-1}{a + j\omega} e^{-(a+j\omega)t} \Big|_0^{\infty} = \frac{1}{a + j\omega} \end{aligned}$$

- **Symmetric Exponential decay**

$$x(t) = e^{-a|t|} \quad (a > 0)$$

As the two-sided exponential decay is the sum of the right and left-sided exponential decays, its spectrum of  $x(t)$  is the sum of their spectra due to linearity:

$$\mathcal{F}[e^{-a|t|}] = \frac{1}{a + j\omega} + \frac{1}{a - j\omega} = \frac{2a}{a^2 + \omega^2}$$

- **Square wave**

A square wave or rectangular function of width  $a$  can be considered as the difference between two unit step functions

$$rect_a(t) = u(t + a) - u(t - a) = \begin{cases} 1 & -a \leq t < a \\ 0 & \text{else} \end{cases}$$

and due to linearity, its Fourier spectrum is the difference between the two corresponding spectra:

$$\begin{aligned} \mathcal{F}[rect_a(t)] &= \mathcal{F}[u(t + a)] - \mathcal{F}[u(t - a)] = \frac{1}{j\omega} e^{ja\omega} - \frac{1}{j\omega} e^{-ja\omega} \\ &= \frac{2}{\omega} \frac{e^{ja\omega} - e^{-ja\omega}}{2j} = \frac{2}{\omega} \sin(a\omega) \end{aligned}$$

- **Sinc function**

The spectrum of an ideal low-pass filter is

$$X(\omega) = \begin{cases} 1 & -a \leq \omega < a \\ 0 & \text{else} \end{cases}$$

and its impulse response can be found by inverse Fourier transform:

$$x(t) = \frac{1}{2\pi} \int_{-\infty}^{\infty} X(\omega)e^{j\omega t} d\omega = \frac{1}{2\pi jt} (e^{jat} - e^{-jat}) = \frac{\sin(at)}{\pi t}$$

### • Gaussian function

The Fourier transform of a Gaussian function  $x(t) = e^{-\pi t^2}$  is

$$\begin{aligned} X(\omega) &= \mathcal{F}[x(t)] = \int_{-\infty}^{\infty} [e^{-\pi t^2}] e^{-j\omega t} dt \\ &= \int_{-\infty}^{\infty} e^{-\pi(t^2 + j2ft)} dt = e^{\pi(jf)^2} \int_{-\infty}^{\infty} e^{-\pi[t^2 + j2ft + (jf)^2]} dt \\ &= e^{-\pi f^2} \int_{-\infty}^{\infty} e^{-\pi(t+jf)^2} d(t+jf) = e^{-\pi f^2} \end{aligned}$$

Here we have used the identity

$$\int_{-\infty}^{\infty} e^{-\pi x^2} dx = 1$$

Thus the Fourier transform of a Gaussian function is also Gaussian:

$$\mathcal{F}[e^{-\pi t^2}] = e^{-\pi f^2}$$

The area underneath either  $x(t)$  or  $X(\omega)$  is unity. Moreover, due to the property of time and frequency scaling, we have:

$$\mathcal{F}[a e^{-\pi(at)^2}] = e^{-\pi(f/a)^2}$$

(If  $a = 1/\sqrt{2\pi\sigma^2}$ , then  $a x(at)$  above is a normal distribution with variance  $\sigma^2$  and mean  $\mu = 0$ .) If we let  $a \rightarrow \infty$ ,  $x(t)$  becomes narrower and taller and approaches  $\delta(t)$ , and its spectrum  $e^{-\pi(f/a)^2}$  becomes wider and approaches constant 1. On the other hand, if we rewrite the above as

$$\mathcal{F}[e^{-\pi(at)^2}] = \frac{1}{a} e^{-\pi(f/a)^2}$$

and let  $a \rightarrow 0$ ,  $x(t)$  approaches 1 and  $X(\omega)$  approaches  $\delta(\omega)$ .

- [1] S. Millman, *A History of Engineering and Science in the Bell System: Communications Sciences (1925-1980)*, AT&T Bell Laboratories, Murray Hill (1984).
- [2] W. F. Brinkman and D. V. Lang, *Physics and the communications industry*, Reviews of Modern Physics, **71**, S480, Centenary 1999.
- [3] R. Wang, *Introduction to Orthogonal Transforms*, Cambridge University Press, New-York (2011).
- [4] E. Bedrosian and S. O. Rice, Proc. of the **IEEE**, **59**, 1688 (1971)
- [5] W. H. Press, W. T. Vetterling, S. A. Teukolsky and B. P. Flannery, *Numerical Recipes in C: The Art of Scientific Computing* Third Edition, Cambridge University Press, New-York (2007).
- [6] G-B Stan, J-J Embrechts and D. Archambeau, *Comparison of Different Impulse Response Measurement Techniques*, J. Audio Eng. Soc., **50**, 249 (2002).
- [7] B. A. Sheno, *Introduction to Digital Signal Processing and Filter Design*, John Wiley & Sons, (2005).
- [8] N. N. Rao, *Fundamentals of Electromagnetics for Electrical and Computer Engineering*, Pearson Education, Inc. Upper Saddle River, New Jersey, 07458 (2009).
- [9] T. H. Lee, *The design of CMOS Radio-Frequency Integrated Circuits*, Cambridge University Press, New-York (1998).
- [10] J-J Werner, **IEEE J. Selected Areas in Communications**, **9**, 785 (1991).
- [11] L. D. Landau and E. M. Lifshitz, *Electrodynamics of Continuous Media*, Pergamon, Oxford (1975).
- [12] D. Zhang, and C. F. Foo, *A Practical Method to Determine Intrinsic Complex Permeabilities and Permittivities for Mn-Zn Ferrites*, **IEEE Trans. Mag.** **41** 1226, (2005)
- [13] T. H. O'Dell, *Circuits for Electronic Instrumentation*, Cambridge University Press, New-York (2005).
- [14] A. I. Talkin and J. V. Cuneo, Rev. Sci. Instr., **28**, 808 (1957).
- [15] A. B. Carlson and P. B. Crilly *Communication systems: An Introduction to Signals and Noise in Electrical Communication*, 5th Edition, McGraw-Hill, New York (2010).
- [16] W. Stallings, *Data and Computer Communications*, tenth edition, Pearson Education, Inc. Upper Saddle River, New Jersey, 07458 (2014).
- [17] I. Kalet and S. Shamai, *On the capacity of a Twisted-Wire pair: Gaussian Model*, **IEEE Trans. Comm.** **38** 379, (1990)
- [18] D.E. Knuth, *The Art of Computer Programming: Semi-numerical Algorithms* Vol. 2, Addison-Wesley (1997).
- [19] P. B Anderson, *Digital Transmission Engineering*, John Wiley & Sons, (2005).